Mechanical and dielectric relaxation studies on the mechanism of oxygen ion diffusion in $La_2Mo_2O_9$

X. P. Wang and Q. F. Fang
Laboratory of Internal Friction and Defects in Solids, Institute of Solid State Physics, Chinese Academy of Sciences, Hefei 230031, People's Republic of China
(Received 9 August 2001; published 10 January 2002)

Both mechanical and dielectric relaxation techniques were applied to investigate the microscopic transport mechanism of oxygen ion and to deduce the dynamical relaxation parameters in oxygen ion conductor $La_2Mo_2O_9$. In the mechanical relaxation measurement, a prominent relaxation peak was observed around 400 K at a measurement frequency of 1 Hz, which is actually composed of two subpeaks (P_1 at lower temperature and P_2 at higher temperature). As for the dielectric experiment, only one relaxation peak was observed above 600 K when the measurement frequency is greater than 500 Hz. The activation energy and the relaxation time at infinite temperature were determined as (0.9 eV, 3×10^{-16} s), (1.1 eV, 2×10^{-16} s), and (0.99 eV, 5×10^{-14} s) for the P_1 peak, P_2 peak, and dielectric peak, respectively. These relaxation parameters are all in the same range as that for oxygen ion diffusion in oxide ceramics, suggesting a mechanism of short diffusion of oxygen ions for the two kinds of relaxation peaks. Based on the crystalline structure of $La_2Mo_2O_9$, an atomistic mechanism of oxygen ion diffusion via vacancies is suggested.

DOI: 10.1103/PhysRevB.65.064304 PACS number(s): 81.05.Je, 66.30.Hs, 62.40.+i, 77.22.Gm

I. INTRODUCTION

Solid electrolytes with a high ionic conductivity of oxygen have been attracting great interest for the applications in fuel cells, oxygen sensors, oxygen pumps, and oxygen-permeable membrane catalysts;[1–6] these devices have the potential to deliver high economic and ecological benefits. In all of these applications the transport of oxygen ions plays a decisive role; it is thus very important to gain a fundamental understanding of the controlling factors that lead to fast ion transport. The fast migration of oxygen ions in a dense crystal lattice is generally observed only in a small number of structural families, such as perovskite, fluorite, intergrowth perovskite/Bi_2O_3, and pyrochlore.[3–8] Recently, Lacorre *et al.*[9,10] reported a new kind of oxygen ion conductor, lanthanum molybdate $La_2Mo_2O_9$ with a cubic structure, which exhibited good oxygen ionic conductivity as high as 0.06 S/cm at 800 °C. In particular, the oxygen vacancies can exist intrinsically in this compound because of the partial oxygen accommodation in its crystal structure, which makes a completely different formation mechanism of oxygen vacancy compared to the traditional solid oxide electrolytes mentioned above. The migration of oxygen ions via vacancies is also responsible for the very good conductivity of $La_2Mo_2O_9$, similar to other kinds of oxygen ion conductors. In $La_2Mo_2O_9$, a high concentration of intrinsic oxygen vacancies can enhance the transport of oxygen ions, which in turn makes $La_2Mo_2O_9$ a good oxygen ion conductor.

The mechanical relaxation (also termed internal friction) technique, which in general measures the dissipation of elastic energy (Q^{-1}), has proved to give valuable information about relaxation dynamics in ceramic samples.[11,12] The dielectric relaxation technique is also a widely used method, which measures the dissipation of electric energy, or the tangent of the loss angle ($\tan\delta$) due to the electric-field-induced reorientation of defects. The combined application of the two techniques has been applied successfully in the study of oxide ceramics such as ZrO_2 and CeO_2.[13] In this investigation, both relaxation techniques were carried out to study the microscopic transport mechanism of oxygen ions and to obtain the kinetic parameters in the oxide-ion conductor $La_2Mo_2O_9$.

II. EXPERIMENTAL PROCEDURE

The polycrystalline ceramic samples of $La_2Mo_2O_9$ used for the present measurements were prepared by the conventional solid-state reaction from a stoichiometric mixture of highly pure La_2O_3 and MO_3 powders. The weighted batches were well mixed, calcined in an alumina crucible at 823 K for 10 h in air. Then the calcined powder was finely ground and pressed into molds to form rectangular samples (about $64\times4\times1.5$ mm^3) for the mechanical relaxation measurements and cylindrical wafers (about 20 mm in diameter and 2 mm in thickness) for the dielectric relaxation measurements. Finally, the pressed samples were sintered at 1223 K for 12 h in air. It is necessary to point out that the two kinds of samples for measurements of both relaxation techniques were prepared in the same procedure and sintered in the same environmental condition, which can help the comparison and analysis of the experimental results obtained from the two different measurement methods.

Mechanical relaxation was measured in a computer-controlled automatic inverted torsion pendulum with the forced-vibration method, in which the measurements at four different frequencies (0.5, 1, 2, and 4 Hz) were carried out by varying the driven frequency in one measurement run with a heating rate of 3 K/min. The maximum torsion strain amplitude was kept at 2.5×10^{-5} in all the measurements.

The samples used in the dielectric experiments were processed into electrodes with silver paste, and the electrodes are connected to the experimental setup through platinum wires. The temperature spectra and frequency spectra of dielectric relaxation were measured using a Hioki 3531 Z Hit-

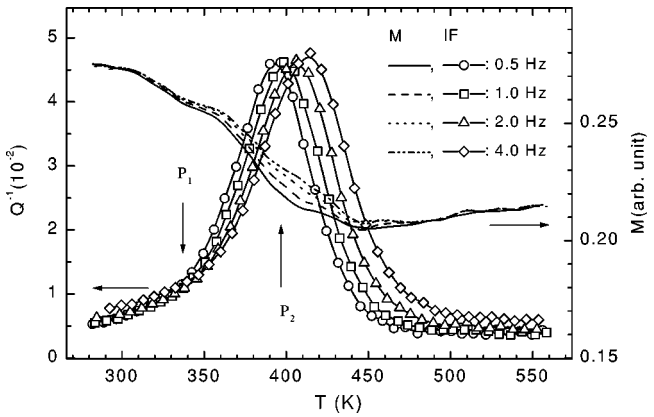

FIG. 1. Temperature dependence of the internal friction (Q^{-1}) and the relative modulus (M) for a $La_2Mo_2O_9$ sample measured at four different frequencies (0.5, 1, 2, and 4 Hz) with a heating rate of 3 K/min.

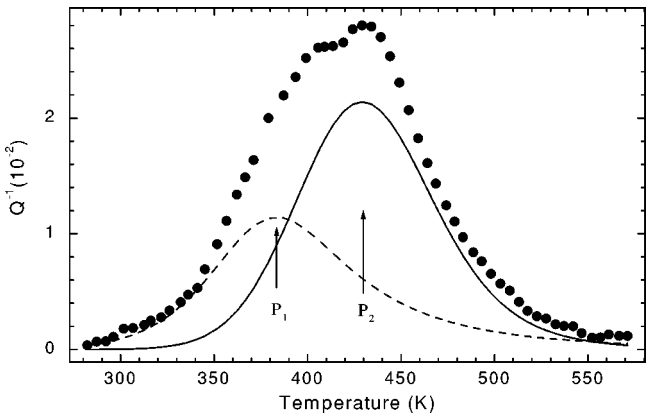

FIG. 2. Temperature dependence of the internal friction (Q^{-1}) for a $La_{1.95}Bi_{0.05}Mo_2O_9$ sample measured at 4 Hz. The circles are experimental data points after the subtraction of the exponential background. The dashed and solid lines are the fitting of the P_1 and P_2 peaks, respectively. Two peaks appear explicitly.

ester instrument made in Japan. This setup operates in a frequency range from 42 Hz to 5 MHz, and the measurable values of the dielectric loss range from 10^{-5} to 10.

III. EXPERIMENTAL RESULTS

A. The measurements of internal friction

Figure 1 shows the internal friction (IF) (Q^{-1}) and the relative modulus (M) versus temperature T in the range from 280 K to 560 K for the oxygen ion conductor $La_2Mo_2O_9$ with a heating rate of 3 K/min at four different frequencies of 0.5, 1, 2, and 4 Hz. A prominent IF peak is observed around 400 K at 1 Hz, accompanied by a corresponding decrease in the modulus. The peak shifts to higher temperature with the increase of frequency, which demonstrates that this peak is associated with a thermally activated relaxation process, whereas the peak height or relaxation strength hardly changes with temperature. With a careful analysis, it can be found that the decrease of the modulus is seemingly composed of two steps centered, respectively, at about 330 K and 400 K at 1 Hz, implying the fine structure of this peak, which has been discussed in detail previously.[14] Accordingly, the IF peak could be well fitted by two Debye peaks with distribution in relaxation time using a nonlinear fitting method,[14] as shown in Fig. 1. The lower-temperature subpeak with a height of 0.005 was denoted by P_1 and the higher-temperature subpeak with a height of 0.04 was denoted by P_2. It is worth noting that the relaxation strength of the P_2 peak was much higher than that of the P_1 peak.

The coexistence of two internal friction peaks (P_1 and P_2 peaks) can be illustrated by the results in a 5% Bi-doped $La_2Mo_2O_9$ sample, where the P_1 peak becomes large enough to show two peaks explicitly. Figure 2 shows the internal friction of a $La_{1.95}Bi_{0.05}Mo_2O_9$ sample as a function of temperature measured at 4 Hz after the subtraction of the exponential background. It can be seen that the main peak (P_2 peak) is located at 430 K. In the lower-temperature side there is a shoulder around 380 K, which indicates clearly the existence of another peak (P_1 peak). Using the same fitting method, P_1 and P_2 peaks are decomposed from the total experimental curve and found to be 0.011 and 0.021 in height, respectively, as shown in Fig. 2. The reason why the P_1 and P_2 peaks appear at higher temperatures and change in height after bismuth doping can be associated with the characteristics of Bi ions. The Bi^{3+} ions have a lone-pair electron that usually occupied a volume similar to that of an O^{2-} anion. This will decrease the free volume in the lattice and hence block the transport of oxygen ions, the details of which will be discussed in another paper.

For a thermally activated relaxation process, the relaxation time τ generally follows the Arrhenius law:[15]

$$\tau = \tau_0 \exp(E/k_B T), \tag{1}$$

where τ_0 is the preexponential factor (or the relaxation time at infinite temperature), T is the absolute temperature, E denotes the activation energy of the relaxation process, and k_B is the Boltzmann constant. It is well known that at the peak position the condition $\omega_p \tau_p = 1$ is fulfilled, where $\omega = 2\pi f$ is the angular frequency of measurement and the subscript p denotes values at peak position. Therefore the relaxation parameters E and τ_0 can be determined from the temperature spectra at different frequencies or from the frequency spectra at different temperatures. If we plot $\ln(\omega_p)$ as a function of the reciprocal of peak temperature (Arrhenius plots), a linear relation would be obtained according to Eq. (1). The so-called Arrhenius plots for the two IF peaks are shown in Fig. 3(a), where the solid lines are the linear least-square fittings. From this figure, the relaxation parameters $E_1 = 1.06$ eV, $\tau_{01} = 1.4 \times 10^{-16}$ s for the P_1 peak and $E_2 = 1.26$ eV, $\tau_{02} = 0.8 \times 10^{-16}$ s for the P_2 peak are obtained from these fitting lines. The values of the relaxation parameters are in the same range as those for oxygen ion diffusion in Y_2O_3-stabilized ZrO_2 (Ref. 11) and in $YBa_2Cu_3O_{7-\delta}$ (Refs. 12 and 16), and comparable with the value deduced from resistance measurements in $La_2Mo_2O_9$, which was 0.9–1.2 eV.[9] This consistency in activation energy suggests a mechanism of short-distance diffusion of oxygen ions via vacancies for P_1 and P_2 peaks.

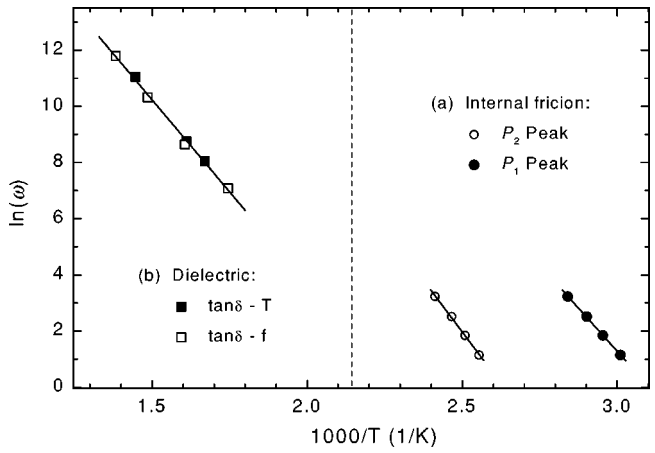

FIG. 3. (a) The Arrhenius plot of the two mechanical relaxation subpeaks (P_1 and P_2 peaks). The relaxation activation energies are $E_1=1.0$ eV for the P_1 peak and $E_2=1.2$ eV for the P_2 peak, respectively. (b) The Arrhenius plot of the dielectric relaxation peak from the spectra in temperature and in frequency. The relaxation activation energy $E_d=1.1$ eV was deduced by calculating the slope of the fitting line.

B. The measurements of dielectric relaxation

The temperature dependence of dielectric relaxation tan δ of the oxygen ion conductor $La_2Mo_2O_9$ is presented in Fig. 4 in the range from 470 K to 760 K. The results are obtained with a heating rate of 3 K/min at three measuring frequencies of 500 Hz, 1 kHz, and 10 kHz. A loss peak superimposed on a large temperature-dependent background is observed at about 600 K when the frequency is equal to 500 Hz. Again the peak height hardly changes with temperature. The peak position apparently shifts to higher temperature with the increase of the measuring frequencies, which indicates that this dielectric peak can be also ascribed to a thermally activated process. For convenience of discussion, we designate this dielectric loss peak as P_d peak.

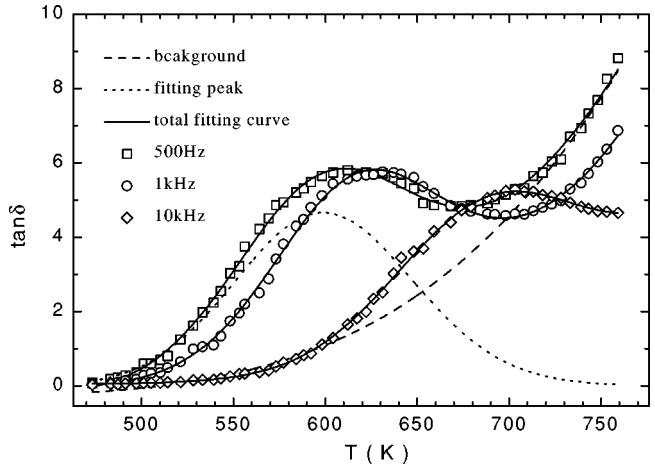

FIG. 4. The variations of dielectric loss with temperature for a $La_2Mo_2O_9$ sample at three different frequencies of 500, 1000, and 10 000 Hz, respectively. The symbols are experimental data points while the solid lines are the total fitting results. The fitting peak (dotted line) and the fitting background (dashed line) are drawn for the results at 500 Hz.

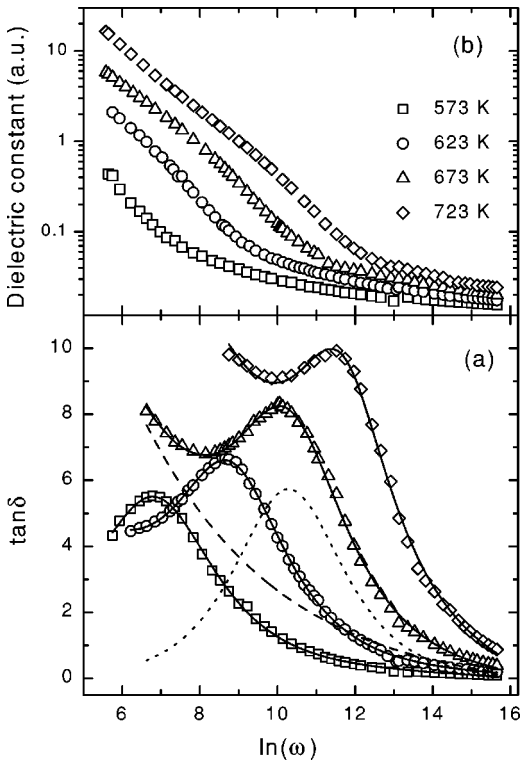

FIG. 5. (a) The curves of dielectric loss versus frequency for a $La_2Mo_2O_9$ sample at four different measuring temperatures of 573, 623, 673, and 723 K, respectively. The symbols are experimental data points while the solid lines are the total fitting results. The fitting peak (dotted line) and the fitting background (dashed line) are drawn for the results at 673 K. (b) The variation of the dynamic dielectric constant in arbitrary units with frequency at the four temperatures.

The relaxation essence of this dielectric peak (P_d) is further confirmed by the fact that a similar peak appears in the curve of the dielectric loss versus frequency. Figures 5(a) and 5(b) show the variation of dielectric loss tan δ and the dynamic dielectric constant with frequency at various temperatures. In this condition, the P_d peak is superimposed on an apparent background increasing with the measuring temperature but decreasing with frequency. The peak position of P_d peak shifts toward higher frequency when temperature increases, and around the peak position the dielectric constant varies dramatically. In solid electrolytes, the conductivity usually increases with the increase of measuring temperature, which will generate additional dielectric dissipation after an electric field is applied[17] and lead to a background increasing with the temperature but decreasing with frequency.

It is worth noting that there is only one peak (P_d peak) in the spectrum of dielectric loss versus temperature or frequency. Using the same nonlinear fitting method mentioned above, the dielectric relaxation spectra of temperature can be well fitted by one Debye peak with a distribution in relaxation time, as shown in Fig. 4, where the details of the fitting results are given only at 500 Hz for clarity. The distribution parameters for the dielectric temperature peak are 0.15 eV for β_H and zero for β_0, where β_0 and β_H are Gaussian distribution parameters that have been defined in detail in our

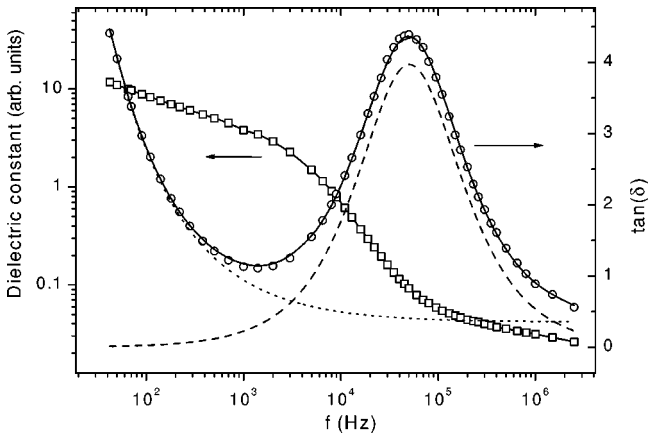

FIG. 6. The variation of dielectric loss and dielectric constant versus frequency at 673 K for a $La_{1.9}Ca_{0.1}Mo_2O_9$ sample. The symbols are experimental data points while the solid lines are the total fitting results. The fitting peak (dashed line) and the fitting background (dotted line) are drawn for the results at 673 K.

previous work.[14] Nonzero β_H and zero β_0 indicate that the dielectric relaxation process has a distribution in activation energy but not in the preexponential factor of the relaxation time.

The complex dielectric constant as a function of frequency can be generally written as

$$\varepsilon_r(\omega)=\varepsilon_r(\infty)+\frac{\varepsilon_r(0)-\varepsilon_r(\infty)}{1+(i\omega\tau)^{1-\alpha}} \tag{2}$$

and thus the dielectric frequency peak can be described as a modified Debye equation,[18]

$$\tan\delta=\frac{(1/2)\Delta\sin(\beta\pi/2)}{\cosh(\beta z)+\cos(\beta\pi/2)} \tag{3}$$

where Δ is the relaxation strength, $z=\ln(\omega\tau)$, $\beta=1-\alpha$, and α $(0\leqslant\alpha<1)$ is the width parameter leading to a symmetric broadening of the Debye relaxation ($\alpha=0$ corresponds to the standard Debye relaxation). The analysis of the curves in Fig. 5(a) with Eq. (3) and an exponential background of $\ln(\omega)$ reveals that there is also only one Debye peak in the frequency spectrum of dielectric loss. The fitting of the curves shown in Fig. 5(a) gives $\beta=0.88$ and $\alpha=0.12$.

The backgrounds in Figs. 4 and 5 vary dramatically in the range of the dielectric loss peak, which will probably increase the difficulty of detecting a small peak such as the P_1 peak. However, this is not the reason why only one peak is observed in the dielectric spectrum, because in a calcium-doped specimen, where the background in the range of the peak is small and varies smoothly, only one peak is detected, as shown in Fig. 6. It can be seen from Fig. 6 that one peak fitting is very satisfactory and there is no trace of another peak. Substituting La^{3+} cations with divalent ions Ca in $La_2Mo_2O_9$ is intentionally applied to maintain the high-temperature phase of $La_2Mo_2O_9$ at low temperature and helps to improve the low-temperature conductivity. In Ca-doped $La_2Mo_2O_9$,[19] two internal friction peaks were also observed as in the undoped $La_2Mo_2O_9$.

From the results shown in Figs. 4 and 5, it is clear that the position of the dielectric peak is closely related to temperature and measuring frequency. The result indicates that the dielectric relaxation is a thermally activated process; the Arrhenius law therefore can be also used to deduce the kinetic parameters of the dielectric relaxation process. According to the shift of the peak position with frequency (for the temperature spectrum) and with temperature (for the frequency spectrum), an activation energy $E_d=1.13$ eV and a preexponential factor of relaxation time $\tau_{0d}=5.0\times10^{-14}$ s are deduced, as shown in Fig. 3(b). The activation energy value of 1.13 eV is close to that for the diffusion of oxygen ions, suggesting that the dielectric relaxation process is associated with oxygen ion diffusion. The difference of the preexponential factors of relaxation time between the mechanical and dielectric relaxation processes is due to the different jump rates of the relaxation species in the mechanical and electrical field.[20]

IV. DISCUSSION AND CONCLUSION

A. Activation parameters of oxygen ion diffusion

From the results presented above, we can see that the relaxation peaks are somewhat broader than a standard Debye peak. This broadening of the relaxation peak is caused by the mutual interaction between the diffusing ions. It is well known that the coupling theory[21,22] is appropriate for phenomenologically describing this kind of mutual interaction. According to this model, the correlation function $C(t)$ is very different in two regions separated by a crossover time t_c, that is, for $t<t_c$,

$$C(t)=\exp(-t/\tau^*), \tag{4}$$

and for $t>t_c$,

$$C(t)=\exp[-(t/\tau)^{1-n}]. \tag{5}$$

Here n is the coupling parameter that can be considered as an indicator of the degree of correlation or cooperativeness in the relaxation process originating from the mutual interactions $(0\leqslant n<1)$, while τ and τ^* are the relaxation times measured experimentally and experienced by an individual ion, respectively. Usually τ and τ^* are not the same and $n\neq0$ in a correlated system. The temperature-independent crossover time t_c in the ionic conductor has an order of magnitude of about 10^{-13} s.[23] Considering the temperature dependence of relaxation time as indicated in Eq. (1), we have the following relations between the experimentally measured parameters (τ_0,E) and the real activation parameters (τ_0^*,E^*):

$$\ln(\tau_0^*)=(1-n)\ln(\tau_0)+n\ln(t_c), \tag{6}$$

$$E^*=(1-n)E. \tag{7}$$

Both parameters n and α describe the broadening of the peak and appear at the same position as an exponent of relaxation time. By comparing Eq. (2) with Eq. (5), the scale in frequency domain $(\omega\tau)$ and in time domain (t/τ) is

TABLE I. The real activation parameters for P_1, P_2, and P_d peaks.

	P_1 peak	P_2 peak	P_d peak
E^* (eV)	0.9	1.1	0.99
τ_0^* (s)	3×10^{-16}	2×10^{-16}	5×10^{-14}

stretched by a factor of $1-\alpha$ and $1-n$, respectively. Because the time domain and frequency domain can be correlated by Fourier transformation, it would be reasonable to assume that the parameter n is equivalent to the parameter α in some aspects. Therefore, we could calculate the parameter α (or n) by fitting the dielectric frequency spectrum with Eq. (3), and then based on Eqs. (6) and (7) and the measured parameters (τ_0, E), calculate the activation parameters (τ_0^*, E^*). In Table I are shown the results of such calculations for P_1, P_2, and P_d peaks, respectively. After such calculations, the activation energy of all the three peaks is around 1.0 eV.

It was reported that the short distance diffusion of oxygen ions via vacancies can lead to a typical mechanical relaxation under periodic stress with an activation energy ranging from 1.0 to 1.5 eV in solid electrolytes.[11,12,16] In our experiments, the activation energy of 1.0 eV for the relaxation peaks is in the same range as that for oxygen ion diffusion in oxide ceramics, which suggests that these relaxation peaks originate from the short distance diffusion of oxygen ions via vacancies.

B. Possible diffusion mechanisms of oxygen ions in the $La_2Mo_2O_9$ crystal

A unit cell of cubic $La_2Mo_2O_9$ crystal ($a=7.1487$ Å) with space group $P2_13$ is shown in Fig. 7, which is based on the refinement results of the x-ray diffraction pattern collected at room temperature using Cu $K\alpha$ radiation. Four La ions and four Mo ions are located near eight corners, with 18 oxygen ions and 10 vacant oxygen sites distributed around them. As a result, in the area around the body center and face centers there is much spare space, which provides possible paths for oxygen ion diffusion. In cubic $La_2Mo_2O_9$ there are three very different kinds of sites for accommodation of oxygen ions, denoted as O(1), O(2), and O(3). Studies using x-ray and neutron diffraction techniques have proved that the O(1) sites are fully occupied but the O(2) and O(3) sites are partially occupied[10] (for example, with occupancy of 87% and 29%, respectively). Since 4a and 12b are the only available sites for space group $P2_13$, other 12b sites are neccessary for accommodation of the extra two oxygen atoms when La, Mo, and O(1) ions occupy the 4a sites and O(2) ions occupy 12b sites. As a result, 14 atoms of O(2) and O(3) will be distributed in 24 possible sites, giving a total occupancy of 59%. If the oxygen deficiency in this system occurs, two 12b sites are still required to accommodate oxygen ions,[10] resulting in a lower occupancy.

The theory of point defect relaxation predicts that relaxation strength has a linear dependence on the defect concentration and the square of the dipole shape factor based on the concept that each point defect (e.g., vacancy) creates an elastic or electric dipole.[15] Considering the high oxygen vacancy concentration in sites of O(2) and O(3), the possibility of migration from O(1), O(2), and O(3) is large enough to produce a relaxation peak with a strength of the order of magnitude of 0.01. According to the thermodynamic selection rule for point defect relaxation, such processes may occur for those point defects whose symmetry is lower than that of the crystal. In the cubic $La_2Mo_2O_9$ crystal, all of the oxygen sites have this lower symmetry. Therefore, an internal friction peak or dielectric loss peak may result from one migration process between the following three pairs when only the jumps between the nearest neighbors are considered:

$$\mathrm{O(1)}\leftrightarrow\mathrm{O(2)} \quad \mathrm{O(1)}\leftrightarrow\mathrm{O(3)} \quad \mathrm{O(2)}\leftrightarrow\mathrm{O(3)}.$$

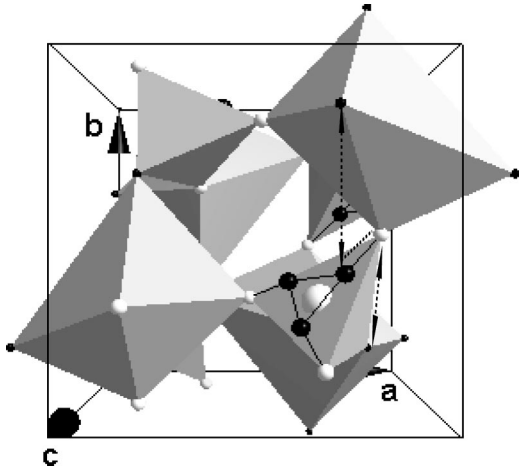

FIG. 7. The crystal structure of the $La_2Mo_2O_9$ oxygen-ion conductor, where the LaO_6 octahedra and the MoO_4 tetrahedra are also shown. The large and small black balls are O(3) and O(1) ions and the large and small white balls are Mo and O(2) ions, respectively. The O(2) and O(3) sites are partially occupied. The possible jump between O(1) and O(2), O(1) and O(3) is shown by dashed arrows. The O(3) ions forming the MoO_7 decahedron are not shown for consideration of clarity.

As shown in Fig. 7, the shortest path of $\mathrm{O(1)}\leftrightarrow\mathrm{O(2)}$ is along the edges of the MoO_4 tetrahedron with a distance of 2.5551 Å, while the shortest path of $\mathrm{O(1)}\leftrightarrow\mathrm{O(3)}$ is between the O(1) ions at the tops of the LaO_6 octahedron and their nearest-neighboring O(3) ions with a distance of 2.6166 Å, as shown by the dashed arrows in Fig. 7. The shortest distance between O(2) and O(3) is about 1.7344 Å as shown by dashed line in Fig. 7, which implies a very small energy barrier between them. Therefore, if the migration between O(2) and O(3) may give rise to a relaxation peak, it would appear at very low temperature or frequency and will be undetectable in the temperature range and the frequency range used in our experiment. Because the vacancy concentration at O(3) sites is much larger than that at O(2) sites, it is reasonable to suggest that the P_2 peak with a much larger relaxation strength may be associated with the short-range diffusion between O(1) and O(3), while the P_1 peak may be related to the diffusion process between O(1) and O(2) via vacancy mechanism. It is worth pointing out

that a long-distance diffusion of oxygen ions may be possible through the path of $O(1)\leftrightarrow O(2)\leftrightarrow O(3)\leftrightarrow O(1)$.

In ceramic oxides, it was reported that the short-range diffusion of oxygen ions or vacancies, similar to the reorientation of the dipole, leads to a dielectric relaxation above 400 K with an activation energy range 0.99–1.12 eV, in which the oxygen ions or vacancies act as polarons.[18] Therefore, the migration processes of oxygen ions mentioned above would give rise to dielectric relaxation peaks when an oscillating electric field is applied. In the present dielectric relaxation measurements, however, only one dielectric relaxation process was observed in oxide-ion conductor $La_2Mo_2O_9$, as shown in Fig. 4. As the activation energy of the P_d peak has a value equal to the average of those of P_1 and P_2 peaks, it is reasonable to suggest that the difference between the two kinds of jumps of $O(1)\leftrightarrow O(3)$ and $O(1)\leftrightarrow O(2)$, which is detected in the case of mechanical relaxation measurements, does not exist in an electric field. In other words, both migration processes of $O(1)\leftrightarrow O(3)$ and $O(1)\leftrightarrow O(2)$ give rise to the same dielectric loss peak, P_d peak. However, to understand the mechanical and dielectric relaxation processes originating from the short-range diffusion of oxygen ions via vacancies in detail, further theoretical analysis based on the crystal structure is necessary.

In summary, we have observed a well-pronounced mechanical relaxation peak in oxide-ion conductor $La_2Mo_2O_9$, which actually consists of two subpeaks, P_1 and P_2. The activation energy and preexponential factor of relaxation time of these two peaks are $E_1=0.9$ eV, $\tau_{01}=3\times10^{-16}$ s for the P_1 peak and $E_2=1.1$ eV, $\tau_{02}=2\times10^{-16}$ s for the P_2 peak. The P_1 and P_2 peaks may originate from two kinds of short-distance diffusion of oxygen ions between different sites, i.e., $O(1)\leftrightarrow O(2)$ and $O(1)\leftrightarrow O(3)$, respectively. However, only one dielectric relaxation peak, the P_d peak, was found in dielectric experiments, The activation parameters for the P_d peak are $E_d=0.99$ eV, $\tau_{0d}=5\times10^{-14}$ s. The P_d peak in the oxide-ion conductor $La_2Mo_2O_9$ may originate from both migration processes of $O(1)\leftrightarrow O(3)$ and $O(1)\leftrightarrow O(2)$. A possible path of long-distance diffusion of oxygen ions may be the jumps of oxygen ions or vacancies from the O(1) site to O(2), then to O(3), and again to O(1), which is three-dimensional in nature.

ACKNOWLEDGMENTS

This work has been subsidized by the National Natural Science Foundation of China (Grant No. 10174083).

[1] H. Yahiro, T. Ohuchi, and K. Eguchi, J. Mater. Sci. **23**, 1036 (1988).
[2] A. Pimenov, J. Ullrich, P. Lunkenheimer, A. Loial, and C.H. Rscher, Solid State Ionics **109**, 111 (1998).
[3] N.Q. Minh, J. Am. Ceram. Soc. **76**, 563 (1993).
[4] K.R. Kendall, C. Navas, J.K. Thomas, and H.C.Z. Loye, Solid State Ionics **82**, 215 (1995).
[5] J.A. Lane, S.J. Benson, D. Waller, and J.A. Kilner, Solid State Ionics **121**, 201 (1999).
[6] J.A. Kilner, Solid State Ionics **13**, 129 (2000).
[7] A.S. Kramer and H.L. Tuller, Solid State Ionics **82**, 15 (1995).
[8] T. Ishihara, H. Matsuda, and Y. Takita, J. Am. Chem. Soc. **116**, 3081 (1994).
[9] P. Lacorre, F. Goutenoire, O. Bohnke, and R. Retoux, Nature (London) **404**, 856 (2000).
[10] F. Goutenoire, O. Isnard, and P. Lacorre, Chem. Mater. **12**, 2575 (2000).
[11] M. Weller and H. Schubert, J. Am. Ceram. Soc. **69**, 573 (1986).
[12] X.M. Xie, T.G. Chen, and Z.L. Wu, Phys. Rev. B **40**, 4549 (1989).
[13] M. Weller, J. Mater. Educ. **17**, 33 (1995).
[14] X.P. Wang and Q.F. Fang, J. Phys.: Condens. Matter **13**, 1641 (2001).
[15] A.S. Nowick and B.S. Berry, *Anelastic Relaxation in Crystalline Solids* (Academic, New York, 1972).
[16] S.J. Rothman, J.L. Roubort, and J.E. Baker, Phys. Rev. B **40**, 8852 (1989).
[17] M. Maglione and M. Belkaoumi, Phys. Rev. B **45**, 2029 (1992).
[18] C. Ang, Z. Yu, and L.E. Cross, Phys. Rev. B **62**, 228 (2000).
[19] X.P. Wang and Q.F. Fang, Solid State Ionics **146**, 185 (2002).
[20] A.S. Nowick and W.R. Heller, Adv. Phys. **14**, 66 (1965).
[21] K.L. Ngai, in *Disorder Effects on Relaxation Processes*, edited by R. Richtert and A. Blumen (Springer-Verlag, Heidelberg, 1994).
[22] K.L. Ngai, Y.N. Wang, and L.B. Magalas, J. Alloys Compd. **211/212**, 327 (1994).
[23] K.L. Ngai and H. Jain, Solid State Ionics **18/19**, 362 (1986).